Heliyon 8 (2022) e09606

Contents lists available at ScienceDirect

Heliyon

journal homepage: www.cell.com/heliyon

Research article

Application and comparison of thermistors and fiber optic temperature sensor reference for ILP measurement of magnetic fluids in double cell magnetic hyperthermia

Sándor Guba [a,*], Barnabás Horváth [a], István Szalai [a,b]

[a] Research Centre for Engineering Sciences, Functional Soft Materials Research Group, University of Pannonia, 10 Egyetem St, H-8200 Veszprém, Hungary
[b] Institute of Mechatronics Engineering and Research, University of Pannonia, 18/A Gasparich Márk St, H-8900 Zalaegerszeg, Hungary

ARTICLE INFO

Keywords:
Magnetic hyperthermia
Differential thermometry
Thermistor
Magnetic fluid
Intrinsic loss power

ABSTRACT

One of the simplest way to characterize the heating efficiency of magnetic fluids used in hyperthermia treatment is the calorimetric measurement of the specific loss power with direct temperature detection. However, the performance of metallic sensors in an alternating magnetic field is degraded by the self-heating of the probes, and electromagnetic interference can be also significant. In our double cell differential thermometric system these disturbing effects can be compensated. Specific loss power measurements of EMG700 magnetic fluid with negative temperature coefficient thermistors in differential configuration are presented, and control measurements were performed with an optical fiber thermometer in $f = 470$ kHz–1020 kHz frequency and $H = 0.13\ \mathrm{kA\,m^{-1}}$–$1.19\ \mathrm{kA\,m^{-1}}$ magnetic field strength range. We found that the specific loss power is proportional to the frequency and shows a quadratic dependence on the field strength in the low field strength region, therefore we calculated the intrinsic loss power of the fluid from the measured specific loss power. At this field conditions intrinsic loss power up to $0.53\ \mathrm{nH\,m^2\,kg^{-1}}$ was determined.

1. Introduction

Colloidal suspensions of magnetic nanoparticles (magnetic fluids) in an alternating (AC) magnetic field with appropriate frequency produce heat mainly due to various relaxation mechanisms (e.g. Néel and Brownian relaxation) [1, 2]. In hyperthermia treatment, these relaxation mechanisms are exploited when a local temperature rise ($T > 42\,^{\circ}\mathrm{C}$) is induced in biological tissues loaded with magnetic nanoparticles (MNPs) [3, 4].

The heating efficiency is quantified by the specific loss power (*SLP*) [5], which gives the power loss of the material normalized by the mass of the magnetic nanoparticles. The value of *SLP* strongly depends on the H amplitude and f frequency of the applied field, but these conditions are equipment specific and vary with different measurement setups. For this reason, the use of the intrinsic loss power (*ILP*) defined as $ILP = SLP/(H^2 f)$ is strongly recommended [6]. This definition is based on the linear response theory (LRT) [7], which can be applied only in a limited range of magnetic field strength, frequency, and core diameter of the magnetic particles. The application of LRT is valid, when there is a linear relationship between magnetization (M) and magnetic field strength, while the particles have a mono-domain structure and show superparamagnetic behavior in the liquid phase. Under these assumptions the *ILP* allows the direct comparison of the heating efficiency of MNPs measured during different field conditions [6, 8].

To determine the power loss, most commonly a non-adiabatic calorimetric method is used [5, 9, 10] because of the complexity of the adiabatic measurement systems [11]. If the temperature rise caused by the alternating magnetic field is measured [12] under non-adiabatic conditions, then the power loss can be calculated from the initial slope ($\left(\frac{dT}{dt}\right|_{t=0}$) of the heating curve as Equation (1) [5]:

$$SLP = \frac{c_p m_{\mathrm{f}}}{m_{\mathrm{MNP}}} \left.\frac{dT}{dt}\right|_{t=0}, \tag{1}$$

where c_p is the specific heat capacity at constant pressure, m_{f} is the mass of the fluid, and m_{MNP} is the mass of the magnetic nanoparticles.

Previously, a double cell thermometric system for laboratory use was proposed to determine the *SLP* values of magnetic fluids with low cost sensors (type K and T thermocouples, and Pt100 resistance temperature detector (RTD)) in differential measurement mode to compensate the self-heating of the sensors [13]. Skumiel and his coworkers [14]

* Corresponding author.
E-mail address: gubas@almos.uni-pannon.hu (S. Guba).

https://doi.org/10.1016/j.heliyon.2022.e09606
Received 16 February 2022; Received in revised form 6 April 2022; Accepted 26 May 2022

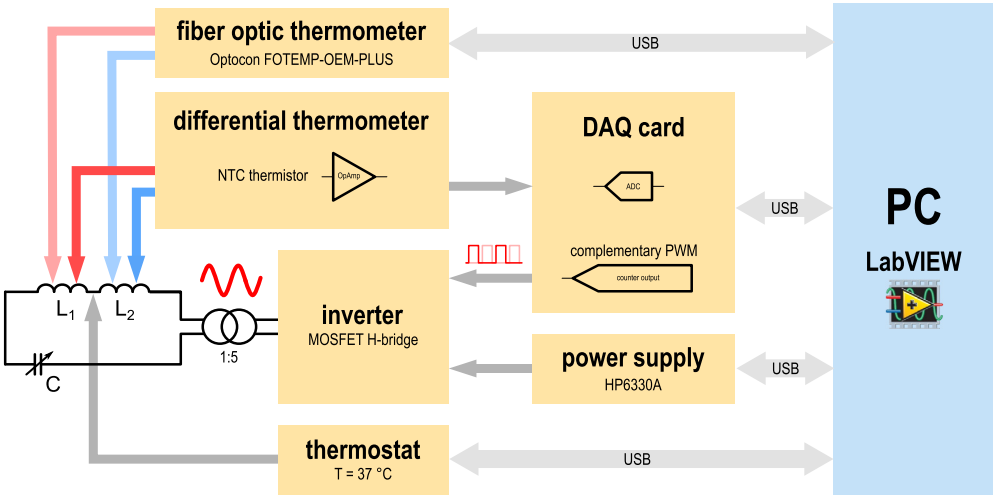

Fig. 1. Block diagram of the double cell calorimetric measurement setup for magnetic hyperthermia.

compared different temperature sensors (including optical fiber sensor and type K thermocouple) to determine the *SLP* values of a magnetic fluid in a single coil measurement system. In this paper first in the literature NTC thermistors are applied in hyperthermia experiments for differential temperature measurement under the influence of external AC magnetic fields. The thermistors are connected as the variable elements of a Wheatstone-bridge, and the differential signal is processed by an instrumentation amplifier to provide high common mode AC rejection. With a modified system the *SLP* is determined in an extended frequency and magnetic field strength range compared to our previous setup. The usability of NTC thermistors in differential configuration was tested under various magnetic field conditions, and the limits of the applicability were also mapped. The NTC thermistors have higher sensitivity to the temperature changes and may be therefore more suitable to detect the heating curves during hyperthermia measurements. Reference measurements were performed using semiconductor based fiber optic thermometer, which is immune to AC magnetic fields. Furthermore, by determining the field strength and frequency dependence of the *SLP* the assumptions used for the definition of *ILP* were tested in the low field strength region.

2. Experimental

2.1. Hyperthermia measurement system

The details of the calorimetric hyperthermia apparatus with differential temperature measurement are given in reference [13]. Here, only the most important aspects and changes made to the system are outlined. The block diagram of the modified complete measurement system is shown in Fig. 1.

Our hyperthermia setup uses a magnetic field generator based on a resonant tank (LC) circuit, which is driven by an inverter circuit. The inverter contains four power transistors (IRF510 power MOSFETs (Vishay)) as switching elements in full H-bridge configuration. The MOSFETs are controlled by two complementary pulse width modulated (PWM) signals with dead time, which are generated by a National Instruments (NI) USB-6221 data acquisition (DAQ) card. The amplifier circuit is fed by a high performance HP6030A power supply.

The LC circuit is made up of two identical hollow core copper tube solenoids (L_1 and L_2) connected in series with a capacitor bank. The temperature of the coils, and therefore the temperature of the sample is kept at a constant $T = 37\,°C$ by circulating thermal fluid through the hollow solenoids. During the recording of the heating curves the $T = 37\,°C$ environmental temperature was the initial temperature to simulate the thermal conditions during clinical treatments. The frequency of the AC field is adjustable between $f = 470$ kHz–1020 kHz by changing the resonant frequency of the LC circuit in discrete steps. This is achieved by replacing the capacitor bank manually. The banks are made of high quality mica capacitors (Cornell Dubilier) to avoid frequency drift due to heating.

The strength of the generated field can be set by limiting the current flowing through the LC circuit, which is measured as a voltage drop over a 0.5 Ω shunt resistor. The magnetic field strength is calculated using the geometry of the coils and the measured current. The maximum peak amplitude of the field is $H_p = 1.19 \pm 0.02\ \mathrm{kA\,m^{-1}}$ at maximum feeding current. For the determination of the *SLP* the low magnetic field strength is beneficial because disturbances are less likely to interfere with the measurement. Most ferrofluids used in medicine have nearly similar particle diameter and this property is consistent with the applicability of *ILP*. Therefore, measurements at low field strengths can be used to extrapolate applicability to clinical conditions. Under clinical treatments the product of frequency and field strength should not exceed $4.85 \times 10^8\ \mathrm{A\,m^{-1}\,s^{-1}}$ (Brezovich criterion) [15]. The operating frequency and field strength range of our apparatus is chosen to remain below or slightly above this limit.

2.2. Differential thermometer

In the differential thermometric system two temperature sensing elements are connected together, forming a differential thermometer. One side is placed into the magnetic fluid sample, while the other side is immersed in a reference material. The basic configuration of our system was described in detail in reference [13]. There were changes in the sensing circuits to adapt to new type of sensing elements such as NTC thermistor. The signal of the sensing circuits were measured by the NI DAQ card.

The differential temperature measurement with NTC thermistor is similar to the differential Pt100 RTD measurement. The sample and the reference thermistors are connected in a Wheatstone-bridge circuit (Fig. 2). The temperature difference between the two sides unbalances the bridge and creates voltage difference which is proportional to the temperature difference. The gain factor of the INA125 (Burr-Brown) instrumentation amplifier is $G = 10$. The resistance of the glass bead NTC thermistors (Tewa) is 10 kΩ with B value of 3950 K. The diameter of the sensor is 1.74 mm. The sensitivity of the differential thermometer with NTC thermistors is significantly larger ($-72.3\ \mathrm{mV\,°C^{-1}}$) than with the previously used type K and T thermocouples and Pt100 RTD sensors ($3.7\ \mathrm{mV\,°C^{-1}}$, $3.8\ \mathrm{mV\,°C^{-1}}$ and $3.7\ \mathrm{mV\,°C^{-1}}$ respectively). Therefore, the heating curves are smoother and the signal noise is below the resolution of the sensor. Thermistors have nonlinear characteristics, but in our

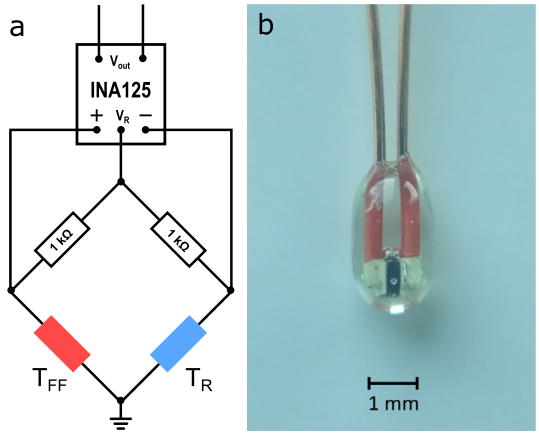

Fig. 2. The NTC thermistor temperature measurement circuit (a). T_{FF} indicates the sensor in the sample side and T_R indicates the sensor in the reference side. One of the NTC thermistor is shown on the right side (b).

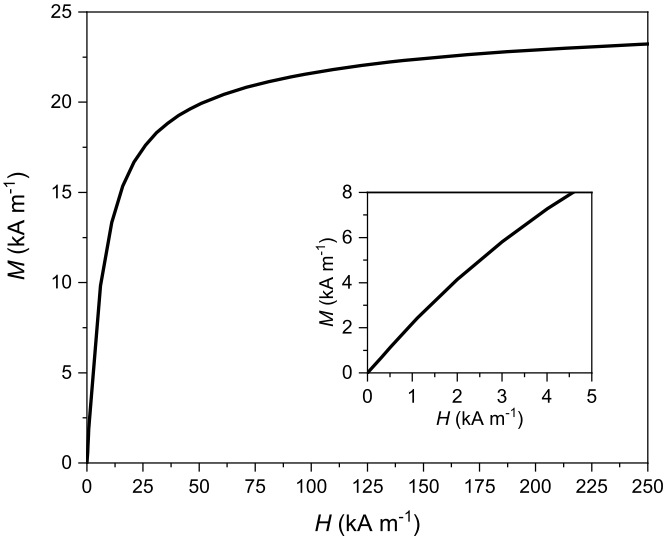

Fig. 3. Magnetization curve of the EMG700 magnetic fluid at $T = 25\,°C$. The inset shows the initial part of the magnetization curve.

case the temperature change is small (under 5 °C) and in this range the nonlinearity of the thermistors does not degrade the accuracy of the differential thermometer compared to thermocouples and Pt100 RTD.

2.3. Materials

For the tests a water based magnetic fluid (EMG700, FerroTec) with a high nanoparticle content was chosen. The magnetization curve of the fluid is shown in Fig. 3, which was measured by a vibrating sample magnetometer (VSM 880, ADE Technologies). It can be seen in the inset graph, that the relationship between M and H is linear in the range of the *SLP* measurements. Furthermore, the absence of remanent magnetization after repeated magnetization cycles indicates a superparamagnetic behavior. The fluid contains magnetite (Fe_3O_4) particles with a nominal diameter of ~ 10 nm (manufacturer data). The volume concentration of the magnetite nanoparticles was 5.8% (manufacturer data). The mass concentration of the nanoparticles was measured by drying method. The calculated mass concentration was 40.6% with relative standard uncertainty of 0.69%. The reference material was distilled water. The volume of the samples and the references in the heating experiments was 3.00 cm^3. The c_p specific heat capacity of the magnetic fluid at $T = 37\,°C$ was 2.900 ± 0.012 $kJ\,°C^{-1}\,kg^{-1}$ (measured with a Setaram C80 differential scanning calorimeter at constant pressure). The relative standard uncertainty of the c_p value is 0.41%. We note, that it is a common practice to assume that the c_p of the fluid equals to the c_p of the carrier liquid at low MNP concentration (in our case $c_{p,water} = 4.18$ $kJ\,°C^{-1}\,kg^{-1}$). However, at higher concentration this assumption is invalid, and can lead to a significant error [16], thus we used the measured c_p values for further calculations.

2.4. SLP calculation

For the calculation of the *SLP* of the magnetic fluid the time dependent heating curves were measured at multiple magnetic field strengths and frequencies. The length of the data collection was around 100 s. The initial slopes were calculated from the first parts of the curves as close as possible to turning on the magnetic field. Because electromagnetic noise transients appeared during the first few seconds of the heating curves this part of the curves were ignored. The $6\ s < t < 80\ s$ interval of the curves was fitted by linear least squares regression, and the initial slope was calculated using this section of the curves. In this interval the heat transfer seemed to be negligible, the curves were linear. Using the measured specific heat capacity at $T = 37\,°C$, the concentration of the MNPs, and the initial slope, the *SLP* of the fluid was determined according to Eq. (1).

In case of every magnetic field strength and frequency three heating curves were recorded. The initial slopes were determined from each curve and their average together with the standard deviation were calculated. To estimate the error of *SLP* determination the combined standard uncertainty of the *SLP* was calculated according the equation in [17] (using the standard uncertainty of the heat capacity measurement and the standard uncertainty of the MNP concentration).

The error of the *ILP* was estimated by calculating the combined standard uncertainty using the uncertainty of the *SLP* determination, the magnetic field strength calculation (3.1%) and the measurement of the frequency (0.21%).

3. Results and discussion

3.1. Self-heating of the temperature probes

In magnetic hyperthermia the performance of metallic sensors in an alternating magnetic field is degraded by the self-heating of the probes [14]. The immunity of the differential thermometer with thermistors to electromagnetic interference and self-heating was tested. Both of the sample and the reference side were filled with distilled water. While one of the sides was in the solenoid the other side was immersed into the water bath of a Huber K6 thermostat to keep the temperature at constant $T = 37\,°C$. In this configuration only one side of the differential thermometer was under the effect of the AC magnetic field. In this case the recorded curve was proportional only to the self-heating. Both of the probes were tested separately in reversed configuration too.

The magnetic field strength was $H_p = 0.44$ $kA\,m^{-1}$ and the frequency was set to 470 kHz during these tests of the sensor elements. The length of the measurement was 10 min. The relative temperature increase was converted into absolute temperature (Fig. 4). Examples from the temperature curves recorded during single measurements of the individual probes and in the differential configuration are shown in Fig. 4.

In case of individual thermistor sensors a temperature increase of 0.13 °C was observed (Fig. 4 (a)). The initial small rise seen in the first few seconds was caused by the fact that the two thermistor sensor elements of the two sides were not perfectly identical, but the symmetry of the two probes was acceptable. The fluctuation on the reference graph was probably caused by the thermostat.

In the differential configuration the effect of self-heating was canceled out; there was no significant temperature change (under 0.04 °C) in differential signal after the initial rise (Fig. 4 (b)).

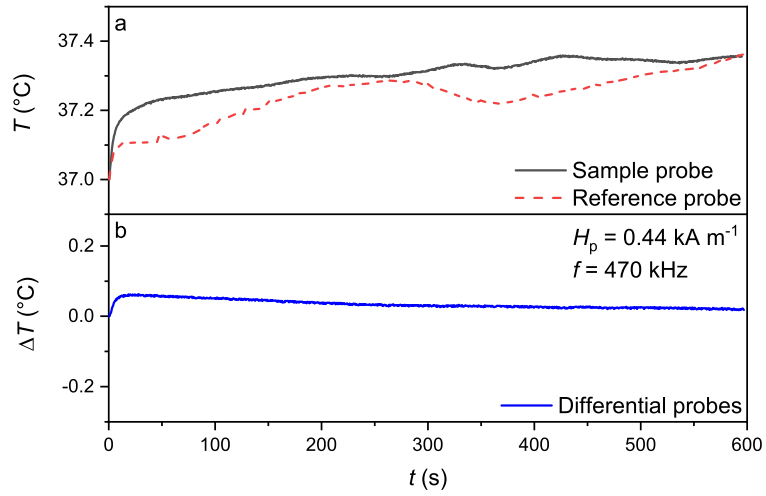

Fig. 4. The individual signals (single measurements) of the sample and reference probes of the differential thermometer using water blanks in case of thermistor probes in a $H_p = 0.44$ kA m^{-1} and $f = 470$ kHz magnetic field (a). The figure on the bottom (b) shows the compensated self-heating in the differential configuration of the same probes in water blanks under the same AC magnetic field.

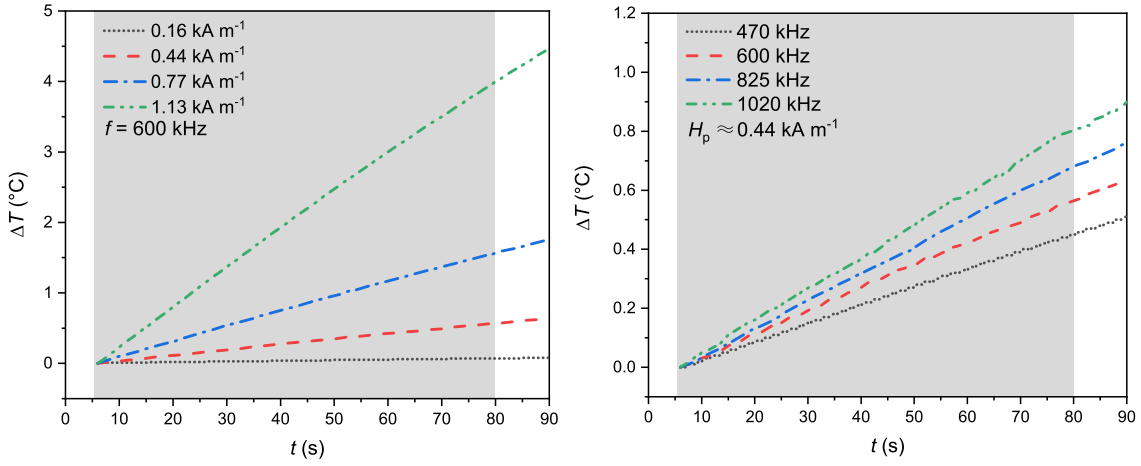

Fig. 5. Single measurement example from the heating curves of EMG700 fluid with the thermistor sensors at $f = 600$ kHz and different field strength (a) and at $H_p \approx 0.44$ kA m^{-1} and different frequencies (b). The gray area indicates the range where the initial slope was calculated. The temperature difference is measured compared to the $T = 37$ °C initial temperature.

3.2. Temperature measurement of the fluid

The temperature increase of the magnetic fluid was recorded in differential mode using the thermistor sensors at different frequencies and magnetic field strengths. Control measurements were conducted with FOTEMP-OEM-PLUS (Weidmann Optocon) thermometer and TS4 fiber optic temperature sensor. The TS4 sensor is based on a GaAs semiconductor crystal.

The magnetic field strength was set between 0.13 kA m^{-1} and 1.19 kA m^{-1} by setting the feeding current of the inverter circuit between 300 mA and 800 mA. The same feeding current at different frequencies results in a slightly different (by 5.5%) field strength value.

3.2.1. Thermistors

In Fig. 5 an example of the recorded heating curves with thermistor sensors is shown at $f = 600$ kHz and different field strength (a) and at $H_p \approx 0.44$ kA m^{-1} and different frequencies (b). The temperature increase was steady and near linear after 6 s in all other frequency and field strength cases too.

Satisfactory measurement results were obtained between 0.13 kA m^{-1} and 0.70 kA m^{-1} at all frequencies. However, at larger frequencies (above 825 kHz) combined with field strength above 0.70 kA m^{-1} the electromagnetic noise becomes significant with increasing frequency even in the differential configuration, and cannot be fully compensated, which limits the usability of the thermistor sensors. If the frequency is limited, then the noise remains acceptable up to the maximum field strength of our setup ($H_p = 1.19$ kA m^{-1}). The specific frequency and magnetic field strength range where the thermistors in differential configuration can work properly is shown in Fig. 6.

The signal noise of the thermistor sensors was lower compared to the previously used thermocouples (Fig. 7). The higher sensitivity of the thermistors enables the detection of smaller temperature changes, which could be an advantage for the measurement of the *SLP* especially at low field strengths.

3.2.2. Fiber optic temperature sensor

Except for the lowest magnetic field strength in all other cases a control measurement was performed with fiber optic temperature sensor. This instrument is immune to electromagnetic interference and self-heating, therefore enables the measurement of temperature under the effect of AC magnetic fields, and can be used as a reference. Although the resolution of the fiber optic thermometer is limited (0.1 °C,

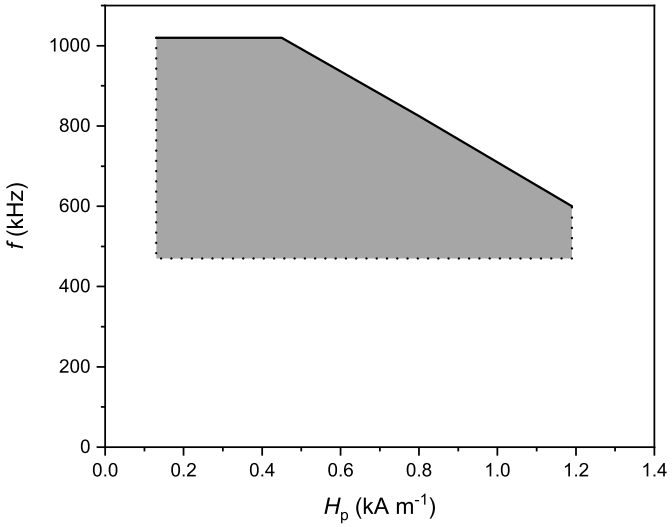

Fig. 6. Usability ranges of the NTC thermistor temperature sensors in differential mode in case of EMG700 fluid. Outside the dotted line no measurements were performed within the framework of this research.

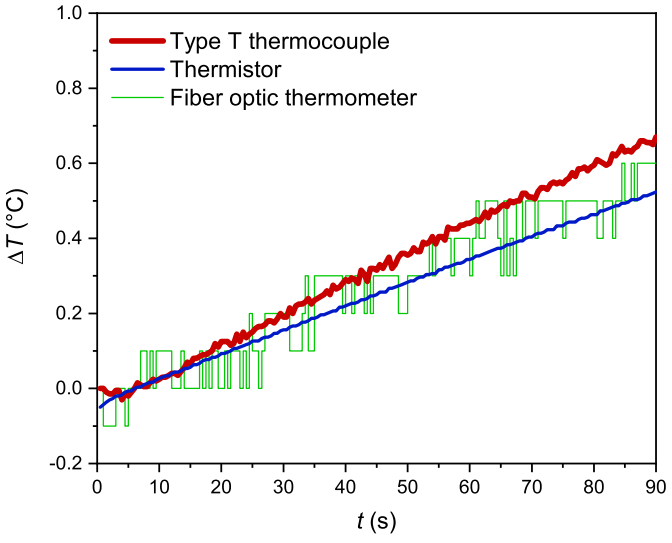

Fig. 7. Comparison of signals of the type T thermocouple, NTC thermistor and fiber optic thermometer. The temperature difference is measured compared to the $T = 37\,°C$ initial temperature.

see Fig. 7), the correlation between the values measured by the optical and thermistor sensors is good (Fig. 8). The sudden rises seen in the curve of the fiber optic sensor were due to the operating characteristics of the instrument, which appeared without the AC magnetic field as well. In case of the lowest magnetic field strengths (below 0.45 kA m^{-1}) the temperature increase was too low to be detected with the resolution of the fiber optic thermometer.

The precise determination of $\frac{dT}{dt}\Big|_{t=0}$ requires a reliable method to record the temperature increase. The resolution (0.1 °C) and the response time (500 ms) of the FOTEMP-OEM-PLUS instrument are common parameters among fiber optic thermometers. In our measurements there was no rapid temperature rise, but at larger field strengths the temperature increase can be multiple times larger. In that case, due to the relatively larger response time, the temperature change cannot be accurately detected by the fiber optic sensor. The problem is similar at small temperature changes: due to the low resolution the linear part of the heating curve is not visible. In case of the lowest magnetic field strength there are no control measurement for the thermistor data due to the above mentioned limitation of the fiber optic thermometer.

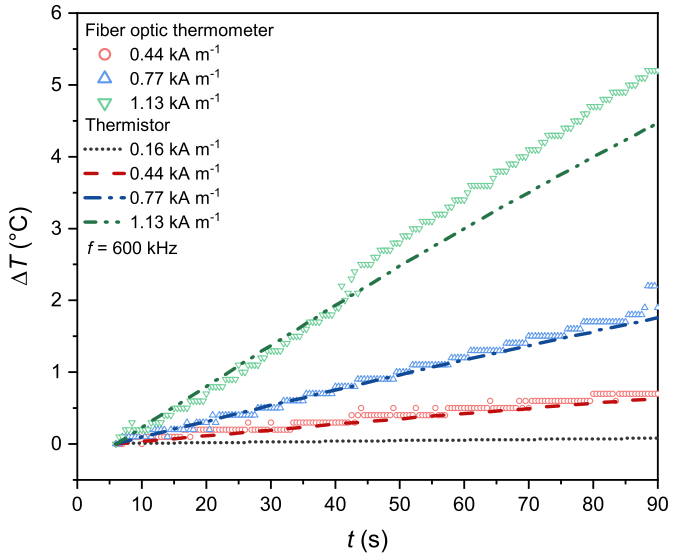

Fig. 8. Comparison of the heating curves measured with the fiber optic thermometer (symbols) and the thermistor sensors (solid lines) at different field strength at $f = 600$ kHz (single measurements). In case of the fiber optic thermometer no measurement was made below 0.44 kA m^{-1}. The temperature difference is measured compared to the $T = 37\,°C$ initial temperature.

3.3. SLP and ILP of the fluid

To calculate the *SLP* values of the fluid Eq. (1) is used. The results are summarized in Table 1 together with the *ILP* data. The average relative error of the $\frac{dT}{dt}\Big|_{t=0}$ calculation is 0.5% (0.4×10^{-4} °C s^{-1}). The values measured with thermistors are slightly smaller (by average of 6.6%) compared to the fiber optic thermometer. Larger deviation is only detected in case of the lowest and the highest frequencies (18.2% and 15.7% respectively). If the results of our previous study obtained with thermocouples and Pt100 RTD thermometer [13] are compared, those values are slightly larger than the present fiber optic thermometer data, the relative difference is 9.4%. The average relative error of the $\frac{dT}{dt}\Big|_{t=0}$ calculation in case of type K and T thermocouples and Pt100 RTD were 1.2%, 0.5% and 1.3% respectively. After normalizing the *SLP* values by the frequency and field strength the resulting *ILP* values became comparable with other studies [6, 8]. The *ILP* values of the EMG700 fluid measured with the thermistor sensors were between 0.34 ± 0.02 nH m^2 kg^{-1} and 0.53 ± 0.03 nH m^2 kg^{-1}, which are characteristic to fluids containing MNPs with a magnetic core diameter smaller than 9.5 nm.

In the definition of the *ILP* it is assumed that the linear response theory can be applied [7, 18] in the appropriate particle size range. As a consequence, the *SLP* of fluids containing small ($d < 10$ nm) MNPs should be proportional with the frequency and would have a quadratic dependence on the amplitude of the magnetic field, as it was shown by Cobianchi and his coworkers [19]. Commonly the *SLP* is measured at larger field strengths up to ~ 20 kA m^{-1}. The use of the *ILP* should be reasonable in the lower field strength regime ($H_p < 1$ kA m^{-1}) too, but it is rarely verified experimentally. Here, the dependence of the *SLP* on f and H_p below 1 kA m^{-1} is tested, and it is found that in case of the EMG700 fluid the linear and quadratic dependence ($SLP \propto H^x$, where $x \approx 2$) holds, respectively (Fig. 9). This behavior is characteristic to other magnetic fluids too, which show superparamagnetic properties. On the other hand, outside the superparamagnetic domain, such as in case of ferromagnetic particles, the field strength dependence deviates from the quadratic relation, as $x > 2$. In this region instead of the LRT the Stoner-Wohlfarth model can be used to evaluate the field strength dependence of the *SLP* [19].

Table 1. The initial slopes of the heating curves and the derived *SLP* and *ILP* values of the EMG700 fluid at different frequencies and magnetic field strength. The values are averages of three individual measurements.

		Thermistor			Fiber optic thermometer		
f (kHz)	H_p (kA m^{-1})	$dT/dt\|_{t=0}$ (°C s^{-1} × 10^{-4})	*SLP* (W g^{-1})	*ILP* (nH m^2 kg^{-1})	$dT/dt\|_{t=0}$ (°C s^{-1} × 10^{-4})	*SLP* (W g^{-1})	*ILP* (nH m^2 kg^{-1})
470	0.15	7.3 ± 0.1	0.005 ± 0.001	0.50 ± 0.03	–	–	–
470	0.44	63.0 ± 0.1	0.045 ± 0.001	0.50 ± 0.03	77.1 ± 6.5	0.055 ± 0.005	0.62 ± 0.07
470	0.75	172.1 ± 0.3	0.123 ± 0.002	0.47 ± 0.03	185.2 ± 6.0	0.132 ± 0.005	0.50 ± 0.04
470	1.15	436.1 ± 1.1	0.312 ± 0.006	0.50 ± 0.03	470.4 ± 5.5	0.336 ± 0.007	0.54 ± 0.04
600	0.16	7.0 ± 0.1	0.005 ± 0.001	0.34 ± 0.02	–	–	–
600	0.44	75.8 ± 0.2	0.054 ± 0.001	0.46 ± 0.03	80.9 ± 3.9	0.058 ± 0.003	0.49 ± 0.04
600	0.77	208.7 ± 0.4	0.149 ± 0.003	0.42 ± 0.03	216.1 ± 4.3	0.155 ± 0.004	0.44 ± 0.03
600	1.13	545.7 ± 1.7	0.390 ± 0.007	0.51 ± 0.03	589.7 ± 1.1	0.422 ± 0.011	0.55 ± 0.04
825	0.14	11.9 ± 0.1	0.009 ± 0.001	0.53 ± 0.03	–	–	–
825	0.40	93.3 ± 0.2	0.067 ± 0.001	0.50 ± 0.03	93.8 ± 4.1	0.067 ± 0.003	0.50 ± 0.04
825	0.70	270.7 ± 0.7	0.194 ± 0.003	0.48 ± 0.03	252.7 ± 4.4	0.181 ± 0.004	0.45 ± 0.03
825	1.19	–	–	–	718.3 ± 13.8	0.514 ± 0.013	0.44 ± 0.03
1020	0.13	9.7 ± 0.1	0.007 ± 0.001	0.38 ± 0.03	–	–	–
1020	0.46	108.2 ± 0.2	0.077 ± 0.001	0.36 ± 0.02	128.4 ± 5.2	0.092 ± 0.004	0.43 ± 0.03
1020	0.70	–	–	–	348.1 ± 4.7	0.249 ± 0.006	0.50 ± 0.03
1020	1.19	–	–	–	1019.5 ± 10.0	0.729 ± 0.015	0.51 ± 0.03

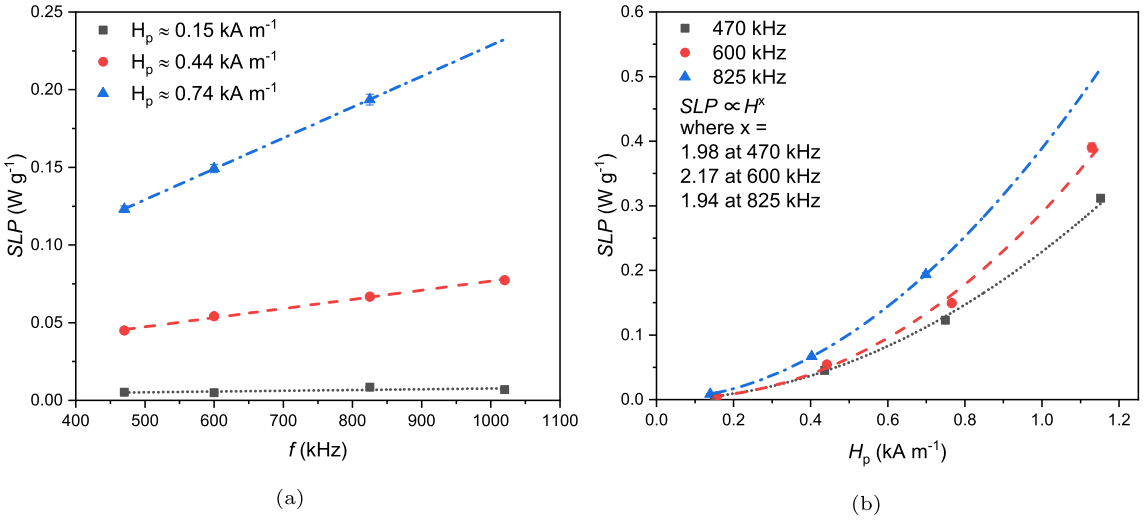

Fig. 9. Curves of the frequency (a) and magnetic field (b) dependence of the *SLP*. Symbols indicate the data points with error bars and the lines indicate the fitted curves. In most cases, error bars are smaller than the symbols. The data points measured at the maximum field strength and frequency are omitted due to the incomplete datasets.

4. Conclusions

- Modification of a previously described double cell calorimetric *SLP* measuring setup with a thermometer based on thermistors in differential configuration has been presented. The measuring system is capable to determine the *SLP*, and through that the *ILP* value of magnetic fluids in wide frequency (470 kHz to 1020 kHz) and magnetic field strength range (0.13 kA m^{-1} and 1.19 kA m^{-1}). With this low magnetic field strength and high frequency, the product of H_p and f is below the Brezovich criterion in the majority of field conditions, where the measurements with the thermistors were made. The frequency of the AC field can be adjusted by manually changing the capacitor bank.
- It was shown that the NTC thermistors in differential mode are suitable for determining the *SLP* value of magnetic fluids. The self heating of the sensors is compensated in the investigated frequency and field strength range, but the electromagnetic interference imposes a limit on the usability at larger field strength combined with larger frequency. The sensitivity of the differential thermometer was improved with the thermistors compared to the previously used thermocouples and RTD.
- Reference measurements were carried out with fiber optic temperature sensor immune to AC magnetic fields. The agreement between values measured by the thermistor and the fiber optic thermometer was good: the average difference between them was 6.6%. However, below 0.45 kA m^{-1} the fiber optic thermometer was not able to detect the small temperature change unlike the thermistor.
- It was found that the dependence of the *SLP* on the frequency and field strength below 1.2 kA m^{-1} is similar to the case of stronger fields. Therefore, it was verified that the use of the *ILP* is acceptable in the investigated frequency and field strength regime too.

Declarations

Author contribution statement

Sándor Guba, Barnabás Horváth: Conceived and designed the experiments; Performed the experiments; Analyzed and interpreted the data; Contributed reagents, materials, analysis tools or data; Wrote the paper.

István Szalai: Analyzed and interpreted the data; Contributed reagents, materials, analysis tools or data.

Funding statement

This work was supported by the TKP2020-NKA-10 project financed under the 2020-4.1.1-TKP2020 Thematic Excellence Programme by the National Research, Development and Innovation Fund of Hungary.

Data availability statement

Data will be made available on request.

Declaration of interests statement

The authors declare no conflict of interest.

Additional information

No additional information is available for this paper.

References

[1] I. Obaidat, B. Issa, Y. Haik, Magnetic properties of magnetic nanoparticles for efficient hyperthermia, Nanomaterials 5 (2015) 63–89.
[2] M. Harabech, J. Leliaert, A. Coene, G. Crevecoeur, D. Van Roost, L. Dupré, The effect of the magnetic nanoparticle's size dependence of the relaxation time constant on the specific loss power of magnetic nanoparticle hyperthermia, J. Magn. Magn. Mater. 426 (2017) 206–210.
[3] D. Ortega, Q.A. Pankhurst, Magnetic hyperthermia, in: P. O'Brien (Ed.), Nanoscience, Royal Society of Chemistry, Cambridge, 2012, pp. 60–88.
[4] S. Mornet, S. Vasseur, F. Grasset, E. Duguet, Magnetic nanoparticle design for medical diagnosis and therapy, J. Mater. Chem. 14 (2004) 2161.
[5] E.A. Périgo, G. Hemery, O. Sandre, D. Ortega, E. Garaio, F. Plazaola, F.J. Teran, Fundamentals and advances in magnetic hyperthermia, Appl. Phys. Rev. 2 (2015) 041302.
[6] M. Kallumadil, M. Tada, T. Nakagawa, M. Abe, P. Southern, Q.A. Pankhurst, Suitability of commercial colloids for magnetic hyperthermia, J. Magn. Magn. Mater. 321 (2009) 1509–1513.
[7] J. Carrey, B. Mehdaoui, M. Respaud, Simple models for dynamic hysteresis loop calculations of magnetic single-domain nanoparticles: application to magnetic hyperthermia optimization, J. Appl. Phys. 109 (2011) 083921.
[8] B. Behdadfar, A. Kermanpur, H. Sadeghi-Aliabadi, M. del, P. Morales, M. Mozaffari, Synthesis of high intrinsic loss power aqueous ferrofluids of iron oxide nanoparticles by citric acid-assisted hydrothermal-reduction route, J. Solid State Chem. 187 (2012) 20–26.
[9] I. Andreu, E. Natividad, Accuracy of available methods for quantifying the heat power generation of nanoparticles for magnetic hyperthermia, Int. J. Hyperth. 29 (2013) 739–751.
[10] M. Coïsson, G. Barrera, F. Celegato, L. Martino, F. Vinai, P. Martino, G. Ferraro, P. Tiberto, Specific absorption rate determination of magnetic nanoparticles through hyperthermia measurements in non-adiabatic conditions, J. Magn. Magn. Mater. 415 (2016) 2–7.
[11] E. Natividad, M. Castro, A. Mediano, Adiabatic vs. non-adiabatic determination of specific absorption rate of ferrofluids, J. Magn. Magn. Mater. 321 (2009) 1497–1500.
[12] R.R. Wildeboer, P. Southern, Q.A. Pankhurst, On the reliable measurement of specific absorption rates and intrinsic loss parameters in magnetic hyperthermia materials, J. Phys. D, Appl. Phys. 47 (2014) 495003.
[13] S. Guba, B. Horváth, G. Molnár, I. Szalai, A double cell differential thermometric system for specific loss power measurements in magnetic hyperthermia, Measurement 169 (2021) 108652.
[14] A. Skumiel, T. Hornowski, A. Józefczak, M. Koralewski, B. Leszczyński, Uses and limitation of different thermometers for measuring heating efficiency of magnetic fluids, Appl. Therm. Eng. 100 (2016) 1308–1318.
[15] S. Dutz, R. Hergt, Magnetic particle hyperthermia – a promising tumour therapy?, Nanotechnology 25 (2014) 452001.
[16] B.B. Lahiri, S. Ranoo, J. Philip, Uncertainties in the estimation of specific absorption rate during radiofrequency alternating magnetic field induced non-adiabatic heating of ferrofluids, J. Phys. D, Appl. Phys. 50 (2017) 455005.
[17] A. Makridis, S. Curto, G.C. van Rhoon, T. Samaras, M. Angelakeris, A standardisation protocol for accurate evaluation of specific loss power in magnetic hyperthermia, J. Phys. D, Appl. Phys. 52 (2019) 255001.
[18] C. Papadopoulos, E.K. Efthimiadou, M. Pissas, D. Fuentes, N. Boukos, V. Psycharis, G. Kordas, V.C. Loukopoulos, G.C. Kagadis, Magnetic fluid hyperthermia simulations in evaluation of SAR calculation methods, Phys. Med. 71 (2020) 39–52.
[19] M. Cobianchi, A. Guerrini, M. Avolio, C. Innocenti, M. Corti, P. Arosio, F. Orsini, C. Sangregorio, A. Lascialfari, Experimental determination of the frequency and field dependence of specific loss power in magnetic fluid hyperthermia, J. Magn. Magn. Mater. 444 (2017) 154–160.